

# Chromophore-Functionalized Gold Nanoparticles

K. GEORGE THOMAS\*<sup>†</sup> AND  
PRASHANT V. KAMAT\*<sup>‡</sup>

*Photosciences and Photonics Division, Regional Research Laboratory (CSIR), Trivandrum 695 019, India, and Notre Dame Radiation Laboratory, Notre Dame, Indiana 46556-0579*

Received February 12, 2003

## ABSTRACT

We report in this Account the design of chromophore-functionalized metal nanoparticles and the detailed investigation of the ground- and excited-state interactions between the metal nanoparticles and the photoactive molecules. The methodologies adopted for organizing chromophore-functionalized gold nanoparticles on two-dimensional surfaces and the mechanistic details of various deactivation channels of the photoexcited chromophores, such as energy and electron transfer to the metal nanoparticle, are presented. The possible applications of such chromophore-functionalized gold nanoparticles in photovoltaics, light-mediated binding and release of biologically important molecules such as amino acid derivatives, and fluorescent display devices are described.

## Introduction

Design of nanostructured materials, with novel physical properties, has emerged as one of the most exciting areas of scientific endeavor in this decade in which chemical research is playing a dominant role. In the nanoscale size regime (1–100 nm), materials show interesting quantum effects. For example, metal and semiconductor nanoparticles possess novel size- and shape-dependent optical, electrical, magnetic, and catalytic properties. The strong plasmon absorption bands observed for metal nanoparticles, arising from the collective oscillation of “roving” electrons on the particle surface, often serves as a probe

Kakkudiyil George Thomas obtained his early education at the Marthoma College (affiliated with the University of Kerala), Thiruvalla, India. He received his master's degree from the University of Pune in 1983, and his Ph.D. in 1989 from the University of Kerala under the supervision of the late Professor K. Saramma. He was a Postdoctoral Research Associate at the Photosciences & Photonics Division of the Regional Research Laboratory (CSIR, Government of India), Trivandrum, India, during 1989–1994, and is working as a Scientist in the same Division since 1994. He has been a Visiting Scientist at the Radiation Laboratory of the University of Notre Dame (1999 and 2003). His research interests are in the areas of photosensitizing dyes, donor–acceptor systems, nanostructured materials, and photo- and electroswitching devices.

Prashant V. Kamat was born in Binaga, India, and got his M.S. (1974) and Ph.D. degrees (1979) from Bombay University. After carrying out postdoctoral research at Boston University and the University of Texas at Austin, he joined the scientific staff at the Notre Dame Radiation Laboratory in 1983. He has been actively involved in nanoparticle research for more than two decades and has published over 250 research and review articles. Currently he is a Senior Scientist at the Radiation Laboratory and Concurrent Professor in the Department of Chemical and Biomolecular Engineering, University of Notre Dame. He is actively involved in utilizing functionalized semiconductor and metal nanostructures and molecular assemblies for light energy conversion, catalysis, and environmental remediation.

to monitor the interaction with surface-bound molecules. The multifaceted characters of inorganic nanomaterials offer a wide range of research and development possibilities in diverse areas of photonics, electronics, material science, catalysis, and biology. (See, for example, refs 1–10 for comprehensive reviews on metal nanoparticles.)

Organized inorganic-organic nanohybrids can be developed by assembling monolayers of organic molecules containing functional groups, such as amines, thiols, isothiocyanates, and silanes, on the three-dimensional surface of metal nanoparticles (Figure 1). Such monolayer-protected metal clusters (MPCs), prepared by adopting the “two-phase extraction” procedure,<sup>11</sup> its modifications by “place exchange reactions”,<sup>5</sup> design of lipid-nanoparticle conjugate materials through electrostatic interaction,<sup>8</sup> and the use of nanoparticle arrays and superstructures as building blocks for the creation of nanocomposite materials<sup>10</sup> and for sensory applications<sup>9</sup> have been reviewed.

Tailoring the optoelectronic properties of metal nanoparticles by organizing chromophores of specific properties and functions on gold nanoparticles can yield photoresponsive organic-inorganic nanohybrid materials. The organization of the densely packed photoresponsive shell encapsulating the nanoparticle core offers exciting opportunities for the design of novel photon-based devices for sensing, switching, and drug delivery. Metal hybrids of organic molecules assembled as two- or three-dimensional architectures provide routes to the design of materials with novel electrical, optical, and photochemical properties. Gold nanoparticles are widely used for bimolecular labeling and as immunoprobes.<sup>12,13</sup>

In this Account we present our recent efforts to understand the surface binding properties of photoreponsive molecules on Au nanoparticles and their excited-state interactions. Possible applications of such systems for the electrochemical modulation of fluorescence, light-mediated binding, and release of biologically important molecules such as amino acid derivatives and as sensitizers for light energy harvesting are also presented.

## Surface Binding Properties of Capped Au Nanoparticles

Surface modification of metal nanoparticles with organic molecules yields highly ordered structures<sup>14,15</sup> and superstructures.<sup>16</sup> The chemical interactions alter the electron density of the metal nanoparticles, thereby directly affecting the absorption of the surface-bound organic moiety as well as the surface plasmon absorption band.<sup>17–19</sup> We have investigated the complexation ability of organic molecules containing functional groups such as amines and isothiocyanates with tetraoctylammonium bromide (TOAB)-capped spherical Au nanoparticles (diameter from

\* To whom correspondence should be addressed. E-mail: pkamat@nd.edu. Web: <http://www.nd.edu/~pkamat>. Tel.: (574) 631-5411. Fax: (574) 631-8068.

<sup>†</sup> Regional Research Laboratory.

<sup>‡</sup> Notre Dame Radiation Laboratory.

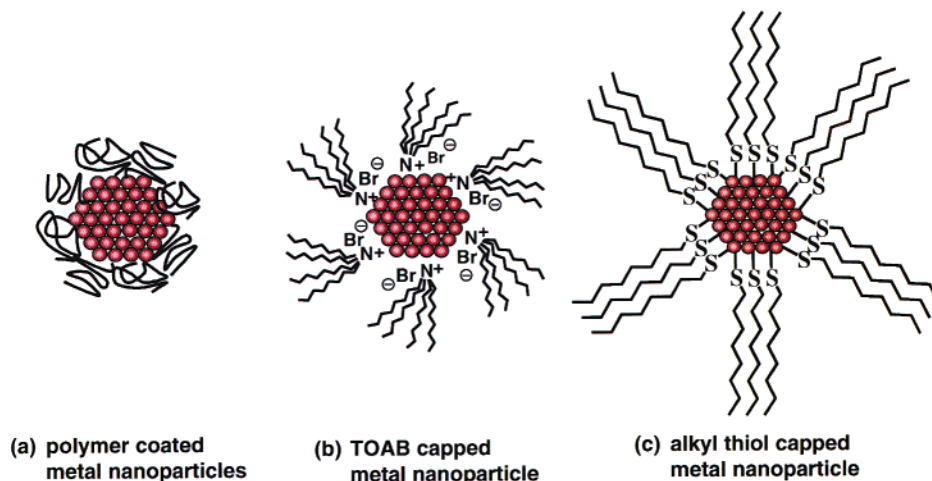


FIGURE 1. Surface functionalization of gold nanoclusters using (a) organic molecules or polymers, (b) quaternary ammonium salts, and (c) alkanethiols.

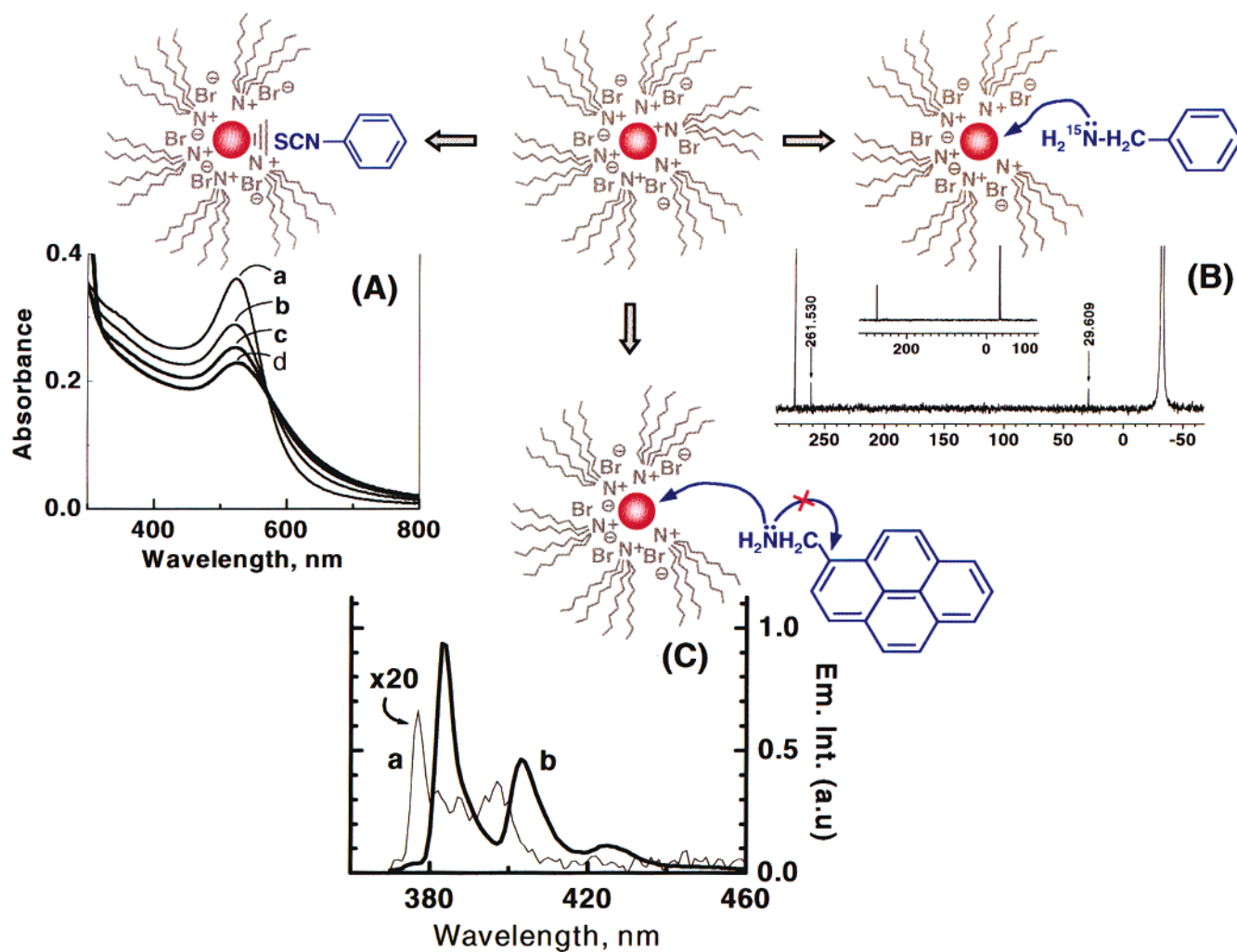


FIGURE 2. (A) Interaction between PITC and gold nanoparticles as probed from the changes in the surface plasmon absorption: (a) 0, (b) 20, (c) 40, and (d) 80  $\mu\text{M}$  PITC. (B) Binding of  $^{15}\text{N}$ -benzylamine with gold nanoparticles as probed by NMR spectroscopy. (C) The effect of binding to gold surface on the emission spectra of 1-methylaminopyrene: (a) no Au and (b) 47  $\mu\text{M}$  gold in toluene. Adapted with permission from refs 20 and 21.

5 to 8 nm). Two model compounds, namely, phenyl isothiocyanate (PITC) and benzylamine, were used to probe the interaction with Au nanoparticles.<sup>20</sup> Both of these compounds were found to alter the absorption

properties of gold nanoparticles; i.e., dampening and broadening of the surface plasmon band were observed, indicative of surface complexation (Figure 2). The high apparent association constant ( $\sim 10^4 \text{ M}^{-1}$ ) indicates strong

association of these molecules on the surfaces of Au nanoparticles. Binding of molecules on nanoparticle surfaces can influence the chemical shifts of the nuclei, and detailed NMR spectroscopic investigations were carried using PITC and  $^{15}\text{N}$ -labeled benzylamine (Figure 2).<sup>20</sup> Complexation of Au nanoparticles with  $^{15}\text{N}$ -labeled benzylamine showed a new signal with a downfield shift of  $\sim 290$  ppm, indicating a strong interaction of the non-bonding electron of the amino group with the surface of the gold nanoparticle. The binding of the amino group to the surfaces of gold nanoparticles was further established by using a fluorescent probe, 1-aminomethylpyrene (Py- $\text{CH}_2\text{NH}_2$ ) (Figure 2).<sup>21</sup> 1-Aminomethylpyrene is weakly fluorescent when dissolved in an organic solvent such as THF, which is attributed to the intramolecular quenching of the singlet excited state via an electron transfer from the lone pair of the nitrogen to the pyrene moiety. However, Py- $\text{CH}_2\text{NH}_2$  bound to gold nanoparticles showed prominent blue emission ( $\phi_F = 0.48$ ) upon illumination with UV light. Binding of the amine group to the gold surface suppresses the intramolecular photoinduced electron-transfer process from the lone pair of the amine to the chromophore, leading to an increase in the efficiency of radiative deactivation of the singlet excited state. Similarly, Katz and co-workers<sup>22</sup> have investigated thioester and thiocarbonate binding to gold using pyrene emission as a probe, and they demonstrated the role of gold in catalyzing thioester and thiocarbonate hydrolysis. Surface-enhanced Raman scattering (SERS) is another sensitive spectroscopic technique, widely used for understanding the interactions between organic molecules and metal nanoclusters<sup>23–26</sup> and widely used in single-molecule detection.<sup>27,28</sup>

**Dye-Capped Metal Nanoclusters.** Noncovalent bonding, such as electrostatic interaction, often leads to close packing of dye molecules on a charged particle surface.<sup>29–31</sup> For silver particles coated with a cationic dye such as Rhodamine 6G, a blue shift was observed for both the silver surface plasmon band and the visible absorption band of the dye.<sup>32</sup> Interestingly, we have observed an H-type aggregation for Rhodamine 6G, when bound to Au nanoparticles with  $\sim 2$  nm diameter.<sup>33</sup> The absorption spectral changes of Rhodamine 6G were investigated in aqueous solution by varying  $[\text{Au}]/[\text{dye}]$  ratios at constant dye concentration ( $4.35 \mu\text{M}$ ) (Figure 3). With increasing  $[\text{Au}]/[\text{dye}]$  ratio, the monomer dye absorption at 525 nm decreased and completely disappeared at a ratio of  $\geq 11$ . Two new bands, corresponding to the dye aggregation band and surface plasmon band of the gold nanoparticles, were observed at 507 and 537 nm (spectra e–g in Figure 3). Although gold nanoparticles of  $\sim 2$  nm diameter do not exhibit any prominent surface plasmon absorption band in the visible region, the clustered aggregates exhibit properties similar to those observed for larger particles (diameter  $> 5$  nm). The gold–dye assemblies coalesce to form larger clusters, due to charge neutralization, resulting in the formation of the dye aggregation band and the gold surface plasmon band. Similarly, surface complexation

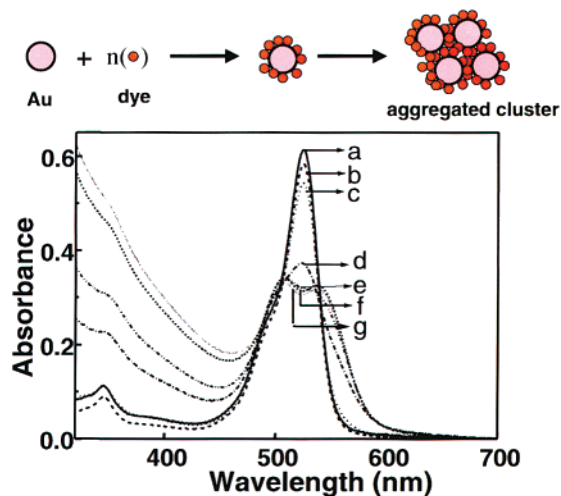


**FIGURE 3.** Absorption spectra of Rhodamine 6G ( $4.35 \mu\text{M}$ ) in aqueous solution containing different concentrations of Au@SCN. The  $[\text{Au}]/[\text{dye}]$  ratio was maintained at values of (a) 0, (b) 0.8, (c) 3.75, (d) 6.0, (e) 11.7, (f) 26.7, and (g) 32.0. Adapted with permission from ref 33.

followed by particle aggregation has been observed for thionicotinamide-capped gold nanoparticles.<sup>19</sup>

## Excited-State Interactions

Close vicinity of a metal nanocore alters the excited deactivation pathways of the surface-bound molecules. For example, Drexhage and co-workers have observed a distance-dependent quenching of excited states of chromophores on metal surfaces.<sup>34</sup> One of the noticeable properties of the fluorophore molecules when bound to metal surfaces is the decreased singlet lifetime as a result of energy transfer from excited dye molecules to bulk metal films.<sup>35–37</sup> Total quenching of the singlet excited states of the chromophores can limit the application of chromophore-labeled metal nanoparticles in optoelectronic devices and photonic materials. Interestingly, recent studies on the photophysical properties of chromophore-linked gold nanoparticle by our group<sup>38,39</sup> and others<sup>40–42</sup> have suggested a dramatic suppression in the quenching of the singlet excited state when these chromophores are densely packed on Au nanoparticle surfaces. A better understanding of the excited-state processes will enable effective utilization of chromophore-functionalized metal nanostructures for light-harvesting and other specialized applications. Possible deactivation pathways of the photoexcited fluorophore bound to a gold nanoparticle, viz., (A) intermolecular interactions, (B) energy transfer, (C) electron transfer, and (D) emission from the chromophores bound on the metal nanoparticles, are summarized in Figure 4. We have examined the possible deactivation pathways of the photoexcited fluorophore bound to Au nanoparticle in detail, and specific examples, which illustrate the excited-state deactivation processes, are discussed below.

**Inter- and Intramolecular Interactions.** To probe the excited-state interactions, we have varied the coverage of the photoresponsive molecule around Au nanoparticle by



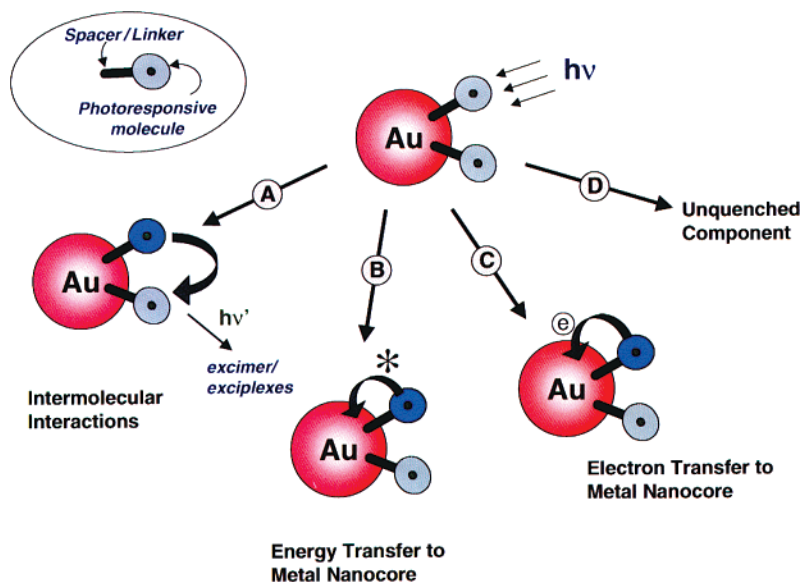


FIGURE 4. Excited-state deactivation processes in fluorophore–metal nanohybrids.

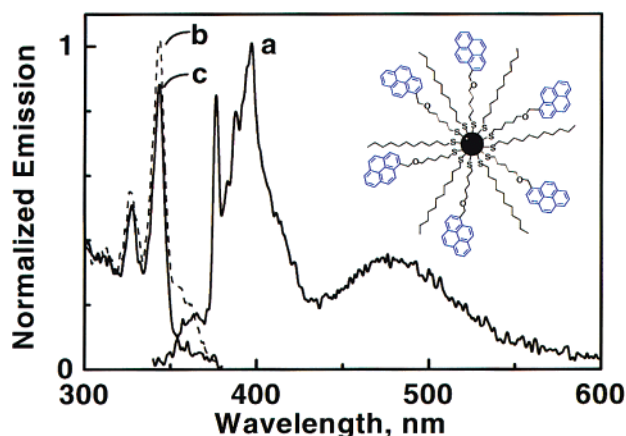


FIGURE 5. (a) Emission spectrum of Au–S–R<sub>1</sub>–Py in THF ( $\lambda_{\text{exc}} = 325$  nm). (b,c) Excitation spectra of Au–S–R<sub>1</sub>–Py in tetrahydrofuran at monitoring wavelengths 390 and 500 nm, respectively. Adapted with permission from ref 38.

co-binding alkanethiols and thiol derivatives of photoresponsive molecules in different proportions. This enabled us to fix the desired number of photoactive molecules around the metal nanoparticle. In a typical preparation, gold nanoparticles capped with thiol derivatives of photoresponsive molecules and alkanethiols were synthesized by reducing HAuCl<sub>4</sub> in the presence of TOAB, adopting a two-phase extraction procedure. The structured absorption bands of pyrene remain more or less unperturbed in pyrene-capped Au nanoparticles (Py–R<sub>1</sub>–S–Au), ruling out the possibility of any ground-state interaction between the chromophore and Au nanoparticle (Figure 5). The fluorescence spectrum of Py–R<sub>1</sub>–S–Au is similar to that of unbound pyrenethiol in THF solution but exhibits noticeably lower yields in polar solvents, indicating that a large fraction of excited pyrene molecules are quenched by the gold nanocore. The intensities of well-structured bands in the absorption (313, 328, and 345 nm) and emission (376, 382, and 395 nm) spectra are often used to sense the polarity of the microenvironment.<sup>43</sup> The

prominence of peak III over peak I (395 nm emission band over 376 nm band) suggests that the pyrene chromophores experience a highly nonpolar microenvironment near the gold surface.

The flexible linker between the nanoparticle and the chromophoric unit provides a topographical control on the interactions between the chromophores in the three-dimensional monolayers. This leads to the formation of the dimer in the excited state, as evident from the excimer emission at 480 nm at higher pyrene loadings. The excitation spectra recorded by monitoring the emission of the monomer (390 nm) and excimer (500 nm) bands confirm that the origin of emission is the same in both cases, viz., excitation of the pyrene chromophores in the Au–S–R<sub>1</sub>–Py assembly.

An example of the conformational mobility of chromophores on cluster surfaces has been illustrated by assembling 6-thiohexyl-3-nitro-4-(4'-stilbenoxymethyl)-benzoate on gold nanoparticle surfaces. These molecules undergo efficient trans-to-cis isomerization but blocked [2 + 2] photodimerization on the nanoparticle surface.<sup>44</sup> In contrast, stilbene derivatives undergo dimerization in self-assembled monolayers (SAMs) on planar gold, indicating that the  $\omega$ -functionalized chromophores on Au nanoparticles are loosely packed. These studies thus conclude that the nature of the linker group provides a topographical control of the various interactions on the three-dimensional surface of metal nanoparticles, leading to the formation of various types of intramolecular complexes.

**Photoinduced Energy Transfer in Organic-Inorganic Nanohybrids.** In many of the examples studied to date, the energy-transfer process is considered to be the major deactivation pathway for excited fluorophores bound on metal surfaces. However, in the case of hybrid assemblies having metal nanoparticles as core, the energy transfer depends critically on the size and shape of the nanoparticle, the distance between the dye molecule and the

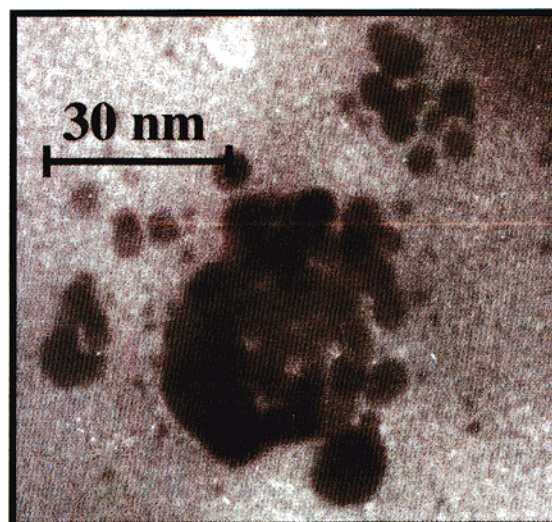
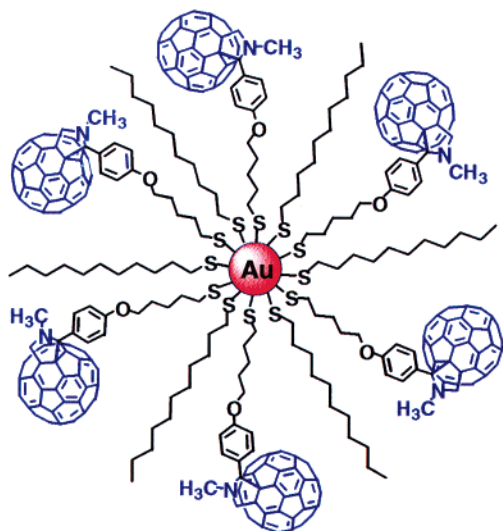


**FIGURE 6.** Transmission electron micrograph of fullerene-thiol/dodecanethiol-bound gold nanoparticles deposited on a copper grid. Adapted with permission from ref 46.

nanoparticle, the orientation of the molecular dipole with respect to the dye–nanoparticle axis, and the overlap of the chromophore emission with the nanoparticle absorption.<sup>45</sup>

We have investigated the excited-state energy-transfer processes in fullerene-functionalized gold clusters ( $C_{60}$ –R–S–Au).<sup>46</sup> Clusters of  $C_{60}$ –R–S–Au can be visualized as antenna systems containing a gold nanoparticle as the central nanocore and appended fullerene moieties as the photoreceptive hydrophobic shell (Figure 6). In the absence of gold nanoparticles, the emission spectrum of fullerene-thiol in toluene showed a maximum at 710 nm, which corresponds to its singlet excited state as reported previously for functionalized  $C_{60}$  molecules.<sup>47,48</sup> In these systems, the major deactivation pathway for the excited singlet is intersystem crossing to generate the triplet excited state. The transmission electron micrographs of Au nanoparticles functionalized with fullerene-thiol ( $C_{60}$ –R–SH) and dodecanethiol showed different size distributions: 10–30 nm diameter for the former one and 1–3 nm for the latter one. A high concentration of fullerenes around a single Au nanoparticle ( $\sim 90$   $C_{60}$  moieties/particle) leads to the formation of small clusters, which further undergo interparticle clustering (it may be noted that fullerenes have a strong tendency for aggregation<sup>49</sup>).

Interestingly, the  $C_{60}$ –R–SH emission is totally quenched when the fullerene is anchored to the gold nanocore. The quenching of singlet emission would result either from enhanced intersystem crossing or by direct energy transfer to the gold nanocore. The low singlet as well as triplet yields of the fullerene moiety in excited  $C_{60}$ –R–S–Au nanohybrids confirm that most of the excited-state energy is quickly dissipated to the Au core via energy transfer.

Light-induced energy-transfer processes from surface-bound chromophores such as  $Ru(bpy)_3^{2+}$ ,<sup>50</sup> fluorenyl derivative,<sup>51</sup> and dansyl derivative<sup>52</sup> to gold nanoparticles have also been reported recently. Dulkeith et al.<sup>45</sup> isolated the resonant energy-transfer rate from the decay rates of excited lissamine dye molecules by chemically attaching

them to gold nanoparticles of different size. The increase in lifetime with decreasing particle size (particle diameter range of 1–30 nm) was indicative of the decreased efficiency of energy transfer in smaller size particles. In a recent study, Heeger and co-workers<sup>53</sup> investigated the role of energy as well as electron transfer in the quenching of emission of conjugated polymers in the presence of gold nanoparticles of varying size. They concluded that resonance energy transfer dominates when the diameter of Au nanoparticle is  $> 2$  nm. Using the principle of energy transfer, attempts are being made to develop biosensors.<sup>54,55</sup> For example, attachment of oligonucleotide molecules labeled with a thiol group at one end of the gold nanoparticle and a fluorophore at the other end has been used to recognize and detect specific types of DNA sequences and single-base mutations in a homogeneous format.<sup>54</sup>

**Photoinduced Electron Transfer in Organic-Inorganic Nanohybrids.** Direct binding of a fluorophore to the metal surface often results in the quenching of excited states.<sup>36,37,56</sup> Indirect evidence for electron transfer between the chromophore and the gold surface has been obtained from photocurrent measurements.<sup>57,58</sup> We have observed that, in polar solvents, pyrene-linked Au nanoparticles ( $Py-R_1-S-Au$ ) exhibit noticeably lower yields compared to unbound pyrenethiol ( $Py-R_1-SH$ ). Time-resolved absorption studies were carried out for establishing the mechanism of quenching.<sup>38</sup> The difference absorption spectrum of unbound  $Py-R_1-SH$  showed a maximum around 425 nm, characteristic of triplet–triplet absorption of pyrene (Figure 7). In contrast, pulsed laser irradiation (337 nm) of  $Py-R_1-S-Au$  nanoparticle, in polar solvents such as tetrahydrofuran, resulted in an electron transfer between the gold nanoparticle and pyrene. The new absorption band at 400 nm confirmed the formation of a pyrene radical cation, which decayed with a lifetime of 4.5  $\mu s$ . The charge-separated states in  $Py-R_1-S-Au$  assemblies are fairly long-lived. The presence of  $O_2$  in the solution had no effect on the formation or decay of this

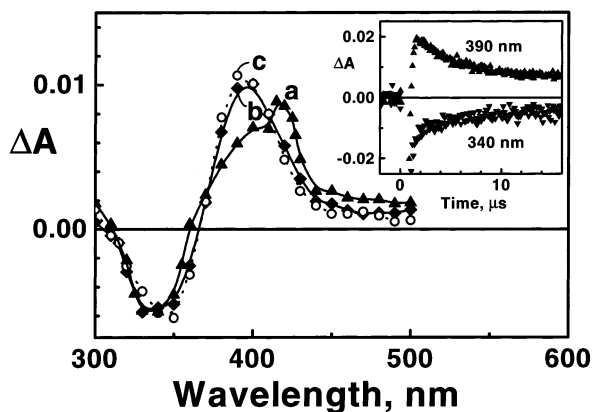


**FIGURE 7.** Transient absorption spectra of (a) degassed THF solution of HS-R<sub>1</sub>-Py, (b) degassed THF solution of Au-S-R<sub>1</sub>-Py, and (c) oxygenated THF solution of Au-S-R<sub>1</sub>-Py. All spectra were recorded 2 μs after 337-nm laser pulse excitation. (Inset) The absorption-time profiles recorded at 400 and 340 nm. Adapted with permission from ref 38.

transient. These observations demonstrate the ability of gold nanoparticles to store and transport electrons.

The decay of the transient absorption at 390 nm and recovery of bleaching at 340 nm (inset, Figure 7) showed a similar first-order kinetics with lifetimes of 4.7 and 4.4 μs, respectively.<sup>38</sup> The similarities between these two processes suggest that the decay of the pyrene cation radical corresponds to the recovery of parent fluorophore via a back electron transfer. As shown earlier, thiol-capped gold nanoparticles are capable of holding the charge in a quantized fashion.<sup>59,60</sup> In an earlier study, transfer of electrons from the excited CdS shell to the gold nanocore

has been demonstrated spectroscopically.<sup>61</sup> The ability of gold nanoparticles to act as a mediator in storing and shuttling the photogenerated electrons demonstrates its usefulness in improving the performance of light-harvesting assemblies.

## Toward Light Energy Harvesting and Other Specialized Applications

**Modulation of Fluorescence of Pyrene-Linked Au Nanohybrids on a Two-Dimensional Surface.** Modification of the gold nanoparticles with fluorophores has important applications in the development of display devices and nanophotonic devices.<sup>4</sup> Furthermore, the electronic properties of surface-bound nanoparticles can be modulated using an externally applied electrical or electrochemical bias.<sup>39,62</sup> The sensitivity of the linker group to the applied potential has been used to arrange quantum dots (CdSe and ZnO) on a conducting substrate.<sup>63</sup>

Controlled charging of the Au nanoassembly has enabled us to modulate the excited-state interaction between the gold nanocore and a surface-bound fluorophore. A bifunctional surface-linking molecule such as mercaptopropionic acid was used to link the gold nanoparticle to the TiO<sub>2</sub> surface (thiol group to gold and carboxylic group to TiO<sub>2</sub>) (Figure 8). Fluorophore-functionalized electrodes were prepared by immersing a TiO<sub>2</sub>-modified conducting electrode (referred as OTE, optically transparent electrode) into the THF solution containing gold nanoparticles that were previously functionalized with mercaptopropionic acid and pyrenethiol (HOOC-

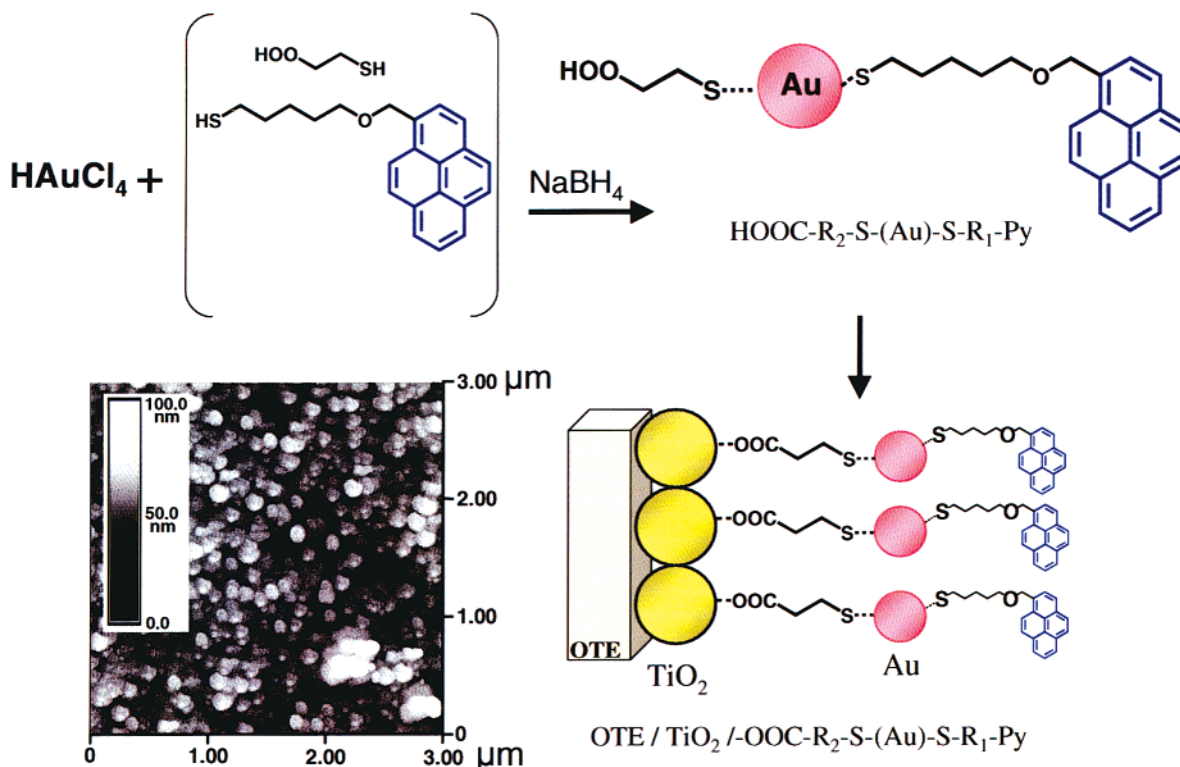


**FIGURE 8.** Binding of fluorophore-linked gold nanoparticles to nanostructured film using a bifunctional surface modifier. Reprinted with permission from ref 39. Copyright 2002 Wiley Interscience Publishers.



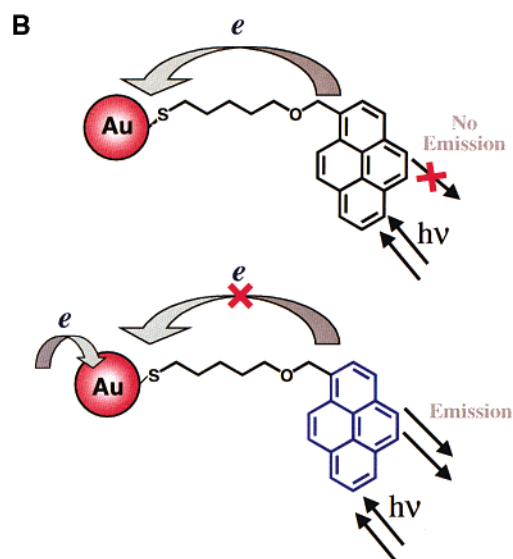
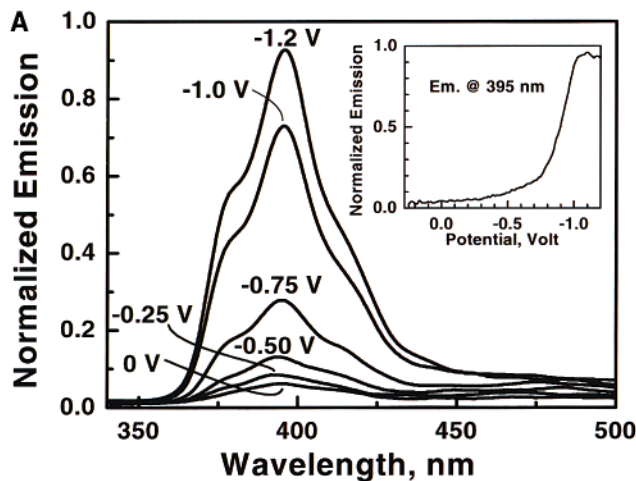
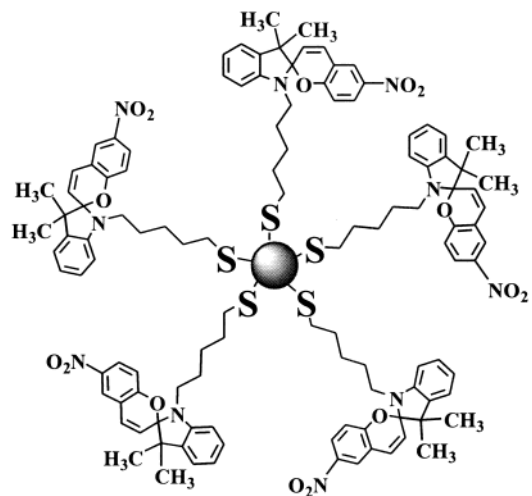


**FIGURE 9.** (A) Emission spectra of OTE/TiO<sub>2</sub>/-OOC-R<sub>2</sub>-S-(Au)-S-R<sub>1</sub>-Py at different applied potentials. Reprinted with permission from ref 39. Copyright 2002 Wiley Interscience Publishers. (B) Excited-state interaction of chromophore with uncharged and charged gold nanoparticles.

R<sub>2</sub>-S-(Au)-S-R<sub>1</sub>-Py).<sup>39</sup> The pyrene-functionalized electrode (referred to as OTE/TiO<sub>2</sub>/-OOC-R<sub>2</sub>-S-(Au)-S-R<sub>1</sub>-Py) exhibits weak emission with a maximum around 395 nm. The decreased singlet lifetime and the formation of the oxidation product (pyrene cation radical) in the Au-S-R<sub>1</sub>-Py assembly indicate the ability of gold nanoparticles to accept electrons from the photoexcited pyrene.<sup>38</sup> Since the oxidation potential of excited pyrene is around -1.5 V versus NHE, one can expect an energetically favorable electron transfer to gold nanoparticles ( $E_T = 0.5$  V).

Spectroelectrochemical experiments carried out using a thin-layer electrochemical cell showed the emission spectra of OTE/TiO<sub>2</sub>/-OOC-R<sub>2</sub>-S-(Au)-S-R<sub>1</sub>-Py electrode at different applied potentials (Figure 9A). As the electrode is biased to negative potentials, an increase in the emission yield was observed. The overall shape of the emission band remains the same, suggesting that the



### Au-SP

**FIGURE 10.** Spiropyran-capped gold nanoparticle (Au-SP).

photoactive molecule contributing to the emission is unperturbed. At potentials more negative than -1.0 V, 90% of the quenched emission is restored by charging the gold nanoparticle (inset, Figure 9A). The quantized charging effects studied with organic-capped gold nanoparticles suggest that the potential shift amounts to about 0.1 V per accumulated electron.<sup>64</sup> The electron transfer from excited pyrene molecules to the gold nanocore experiences a barrier as we charge them with negative electrochemical bias (Figure 9B).

**Light-Mediated Binding and Release of Amino Acid Derivatives.** Chemical linkage of biologically relevant molecules such as proteins, peptides, carbohydrates, lipids, and DNA to gold nanoparticles has led to the development of novel probes for biochemical investigation, with better sensitivity and greater penetration through tissues.<sup>65-67</sup>

We have recently reported the design of a photoswitchable double-shell structure on Au nanoparticle, by anchoring spiropyran (SP) to the three-dimensional surface of Au nanoparticles (Figure 10).<sup>68</sup> The light-regulated changes in the topographic properties of spiropyran-capped Au nanoparticles (i.e., interconversion between the zwitterionic and neutral forms) were exploited for the assembly and release of amino acids (Figure 11) such as L-tryptophan, L-tyrosine, L-DOPA, and  $\alpha$ -methyl-L-DOPA (note that L-DOPA is effective for the treatment of Parkinson's disease and hypertension).

The rationale behind the design of light-mediated self-assembly is based on the fact that the discrete photoisomeric states of spiropyran exhibit distinctly different physical properties. Under dark conditions, the majority of spiropyran molecules exist in their "closed" spiro form (colorless and nonpolar). When excited with UV light, spiropyran undergo photoisomerization to the "open" merocyanine form (highly polar and zwitterionic), absorbing in the visible region. The ring closure to the spiropyran form can occur either thermally or by exposure to visible radiation, and several novel applications have been con-

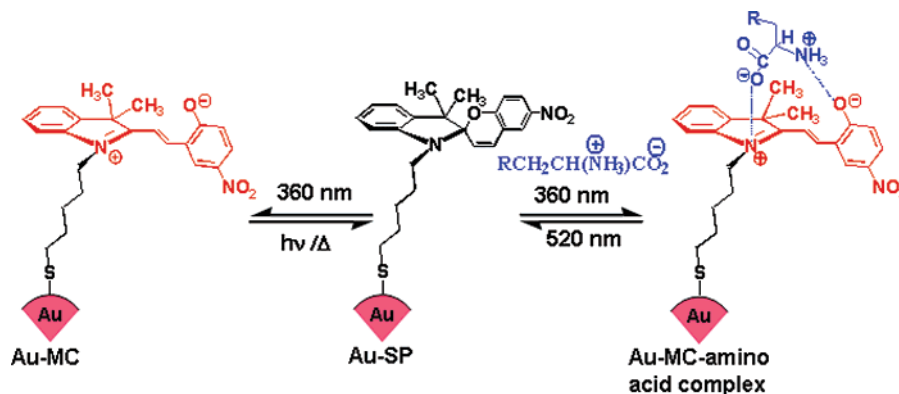


FIGURE 11. Schematic representation of photochemical ring opening and ring closing of **Au-SP** in the absence and in the presence of amino acids. Adapted with permission from ref 68.

sidered by exploiting the light-mediated changes in their physical properties (see articles cited in ref 68). Irradiation of **Au-SP** ( $\sim 130$  SP moieties/particle) in methanol resulted in the formation of an absorption band around 500 nm, which corresponds to the formation of the zwitterionic merocyanine form (**Au-MC**).<sup>68</sup> In the presence of amino acids, an initial decrease in the intensity of the visible absorption band was observed and the absorbance persisted, indicating the stabilization of the zwitterionic merocyanine form.

The two-point electrostatic interaction between the zwitterionic merocyanine on Au nanoparticles and amino acid derivatives results in the formation of a relatively stable complex (e.g., half-life ( $\tau_{1/2}$ ) of **Au-MC**: : : tyrosine complex is  $\sim 14$  h, whereas the  $\tau_{1/2}$  of **Au-MC**  $\rightarrow$  **Au-SP** is 23 min). The **Au-MC**: : : amino acid complex dissociates on photoirradiation at 520 nm and undergoes thermal ring closure to **Au-SP**, releasing the amino acid derivatives. The complexation/dissociation cycles could be repeated many times. Light-mediated binding and release of molecules of amino acid derivatives on the nanoparticle scaffold, in combination with the site specificity of the Au nanoparticle, offers a unique possibility of designing light-mediated controlled release systems.

**Photocurrent Generation.** The fluorophore-modified gold nanoclusters assembled as films on a conducting electrode surface serve as photoresponsive electrodes. The linking of fluorophore-bound gold nanoparticles to nanostructured  $\text{SnO}_2$  (OTE/ $\text{SnO}_2$ ) or  $\text{TiO}_2$  (OTE/ $\text{TiO}_2$ ) films via a bifunctional linker provides an excellent choice to achieve this goal. Using this strategy, we successfully employed OTE/ $\text{SnO}_2$ /pyrene and OTE/ $\text{SnO}_2$ /Au-S-R- $\text{C}_{60}$  as the photoanodes in a photoelectrochemical cell. Upon illumination of these electrodes with visible light ( $\lambda > 400$  nm), a prompt generation of photocurrent could be seen.

The photocurrent action spectra of OTE/ $\text{SnO}_2$  and OTE/ $\text{SnO}_2$ /Au-S-R- $\text{C}_{60}$  electrodes are shown in Figure 12 (traces c and d). Only the electrode OTE/ $\text{SnO}_2$ /Au-S-R- $\text{C}_{60}$  shows a prominent response in the visible (400–500 nm), thereby confirming the role of fullerene moieties as the receptor of incident photons. Repeated ON–OFF cycles of illumination show the reproducibility of a steady photovoltage ( $\sim 150$  mV) and short-circuit photocurrent ( $130 \mu\text{A}/\text{cm}^2$ ) generation. Similarly, photocurrent genera-

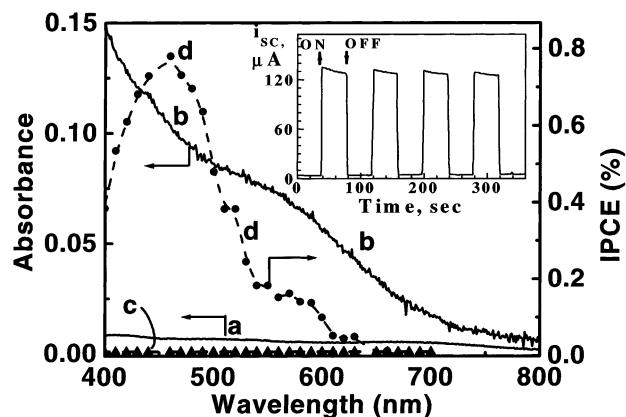


FIGURE 12. Absorption (—) and photocurrent (---) action spectra of (a,b) OTE/ $\text{SnO}_2$  and (c,d) OTE/ $\text{SnO}_2$ /Au-S- $\text{C}_{60}$  electrodes (electrolyte:  $\text{LiI}$  (0.5 M) and  $\text{I}_2$  (0.01 M) in acetonitrile). Incident photon to photocurrent generation efficiency (IPCE) was determined from the expression,  $\text{IPCE} (\%) = 1240(i_{\text{sc}}/i_{\text{inc}})(1240/\lambda)$ , where  $i_{\text{sc}}$  ( $\text{mA}/\text{cm}^2$ ) is the short-circuit current and  $i_{\text{inc}}$  ( $\text{mW}/\text{cm}^2$ ) is the incident light energy at the excitation wavelength,  $\lambda$  (nm). (Inset) The photocurrent response to ON–OFF cycles of illumination ( $\lambda > 400$  nm). Adapted with permission from ref 46.

tion can be observed upon excitation (380–420 nm) of the OTE/ $\text{TiO}_2$ /Au-S- $\text{R}_1$ -Py electrode. Attempts have also been made to immobilize viologen-linked Ru(II) bipyridyl complex bound to gold nanoparticles and Zn(II)–porphyrin–bipyridinium dyad<sup>69</sup> and Au–nanoparticle superstructures on conductive surfaces.<sup>70</sup>

Two distinctively different mechanisms (viz., photo-galvanic and photosensitization processes) can be operative in the anodic photocurrent generation (Figure 13). In the case of fullerene-bound gold nanoparticles, a photo-galvanic process is operative, as the excited fullerene moieties do not participate in the direct charge injection process; instead, they get reduced by charge-transfer interaction with the redox couple. The  $\text{C}_{60}$  anion then injects electrons into gold nanoparticles to generate photocurrent. As shown earlier,<sup>71</sup> the fullerene anions are electroactive and are capable of delivering charges to the collecting electrode surface. A similar mechanism is also operative in the tris(2,2'-bipyridine)Ru(II)–viologen dyad molecule linked to gold nanoparticles.<sup>69</sup> On the other hand, pyrene, having a relatively high excited-state oxida-



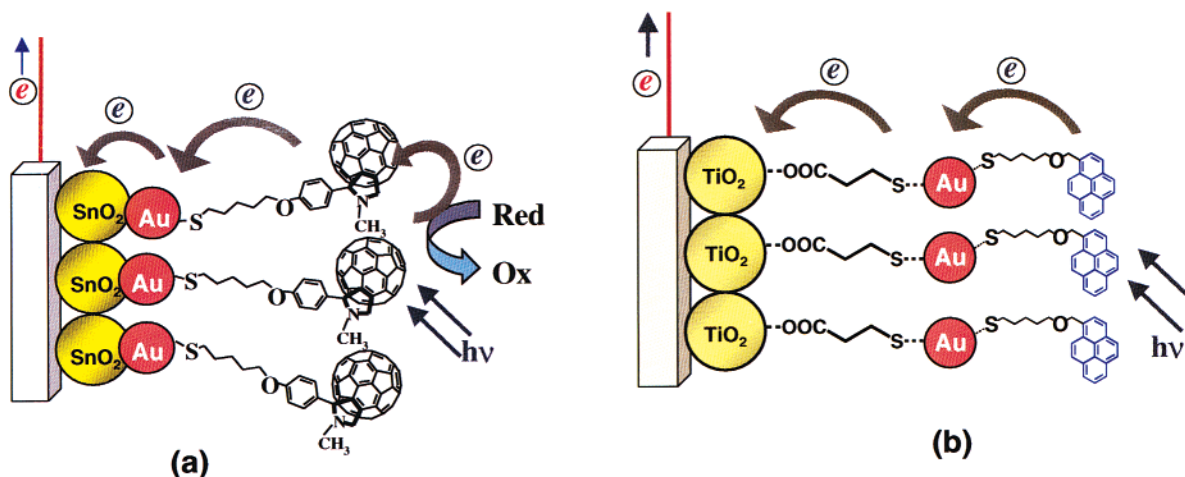


FIGURE 13. Photocurrent generation mechanism based on (a) photogalvanic and (b) photosensitization principles.

#### Exploiting the photochemistry of chromophore functionalized metal nanoparticles

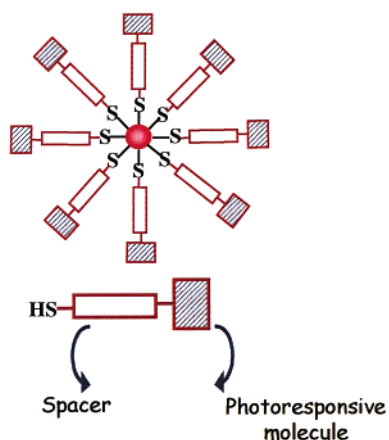


FIGURE 14. Photoresponsive organic-inorganic nanohybrid material.

tion potential, undergoes direct electron transfer with the gold nanoparticles. Following their injection into gold nanoparticles, electrons are transported to the collecting OTE surface to generate the photocurrent. Whether it is photosensitization or photogalvanic mode, the gold nanocores have the unique ability to promote the charge separation and facilitate electron transport within the film during the photocurrent generation.

## Future Directions

The key to creation of organic-inorganic nanohybrids is to understand their chemistry at a fundamental level. The fluorophore-bound metal nanoparticles provide a convenient way to probe the interaction between a metal core and the photoexcited molecule. The examples presented in this Account show the unique properties of metal nanoparticles in modulating the photophysics of a surface-bound fluorophore. The ability of gold nanoparticles in storing and shuttling of electrons, as demonstrated by molecule-like charging effects,<sup>59,64</sup> is an important aspect that needs to be explored fully. It is also important to establish the particle size and distance dependence on the

interaction between excited chromophore and metal nanocore using ultrafast spectroscopy techniques.

Novel methodologies of assembling fluorophore-gold nanohybrids as three-dimensional arrays should facilitate the design of a new generation of nanophotonic and optoelectronic materials, such as in display applications. Photoresponsive organic-inorganic nanohybrid materials are likely to serve as a useful paradigm for sensor and controlled release systems (Figure 14). The mechanism of charge transport in metal nanostructures has remained an intriguing issue, and Brust and co-workers<sup>72</sup> have proposed a thermally activated electron hopping from one gold particle to another as a possible way of conducting charge through nanostructured gold films. The photoelectrochemical response of fullerene-functionalized nanostructured films demonstrates that the gold nanocores can play an important role of mediating the charge transport process in nanostructured electrodes. Though many issues are still being debated, the general interest in organic-inorganic nanohybrids is expected to grow in the coming years.

*The work described herein was supported by the Office of Basic Energy Sciences of the U.S. Department of Energy. This is Contribution No. 4440 from the Notre Dame Radiation Laboratory and PPD-(RRLT)-165 from the RRL, India. K.G.T. thanks the Council of Scientific and Industrial Research (CSIR) and the Department of Science and Technology (DST Grant No. SP/S1/G-21/97), Government of India, for financial support. We would like to thank the members of our research group, N. Chandrasekharan, S. Barazzouk, B. I. Ipe, and P. K. Sudeep, for their active contributions.*

## References

- (1) Kamat, P. V. Photophysical, photochemical and photocatalytic aspects of metal nanoparticles. *J. Phys. Chem. B* **2002**, *106*, 7729–7744.
- (2) Kamat, P. V. Photoinduced Transformations in Semiconductor–Metal Nanocomposite Assemblies. *Pure Appl. Chem.* **2002**, *74*, 1693–1706.
- (3) Markovich, G.; Collier, C. P.; Henrichs, S. E.; Remacle, F.; Levine, R. D.; Heath, J. R. Architectonic Quantum Dot Solids. *Acc. Chem. Res.* **1999**, *32*, 415–423.
- (4) McConnell, W. P.; Novak, J. P.; Brousseau, L. C., III; Fuierer, R. R.; Tenent, R. C.; Feldheim, D. L. Electronic and Optical Properties of Chemically Modified Metal Nanoparticles and Molecularly

- Bridged Nanoparticle Arrays. *J. Phys. Chem. B* **2000**, *104*, 8925–8930.
- (5) Templeton, A. C.; Wuelfing, W. P.; Murray, R. W. Monolayer protected cluster molecules. *Acc. Chem. Res.* **2000**, *33*, 27–36.
  - (6) George Thomas, K.; Ipe, B. I.; Sudeep, P. K. Photochemistry of chromophore-functionalized gold nanoparticles. *Pure Appl. Chem.* **2002**, *74*, 1731–1738.
  - (7) Rao, C. N. R.; Kulkarni, G. U.; Thomas, P. J.; Edwards, P. P. Size-dependent chemistry: Properties of nanocrystals. *Chem.-Eur. J.* **2002**, *8*, 29–35.
  - (8) Sastry, M.; Rao, M.; Ganesh, K. N. Electrostatic assembly of nanoparticles and biomacromolecules. *Acc. Chem. Res.* **2002**, *35*, 847–855.
  - (9) Shipway, A. N.; Katz, E.; Willner, I. Nanoparticle arrays on surfaces for electronic, optical, and sensor applications. *ChemPhysChem* **2000**, *1*, 18–52.
  - (10) Shenhar, R.; Rotello, V. M. Nanoparticles: Scaffolds and Building Blocks. *Acc. Chem. Res.* **2003**, *36*, 549–561.
  - (11) Brust, M.; Fink, J.; Bethell, D.; Schiffrin, D. J.; Kiely, C. Synthesis and reactions of functionalized gold nanoparticles. *J. Chem. Soc., Chem. Commun.* **1995**, 1655–1656.
  - (12) Ribrioux, S.; Kleymann, G.; Haase, W.; Heitmann, K.; Ostermeier, C.; Michel, H. Use of Nanogold- and Fluorescent-labeled Antibody Fv Fragments in Immunocytochemistry. *J. Histochem. Cytochem.* **1996**, *44*, 207–213.
  - (13) Elghanian, R.; Storhoff, J. J.; Mucic, R. C.; Letsinger, R. L.; Mirkin, C. A. Selective Colorimetric Detection of Polynucleotides Based on the Distance-Dependent Optical Properties of Gold Nanoparticles. *Science* **1997**, *277*, 1078–1081.
  - (14) Fink, J.; Kiely, C.; Bethell, D.; Schiffrin, D. J. Self-organization of nanosized gold particles. *Chem. Mater.* **1998**, *10*, 922–926.
  - (15) Novak, J. P.; Brousseau, L. C.; Vance, F. W.; Johnson, R. C.; Lemon, B. I.; Hupp, J. T.; Feldheim, D. L. Nonlinear optical properties of molecularly bridged gold nanoparticle arrays. *J. Am. Chem. Soc.* **2000**, *122*, 12029–12030.
  - (16) Sarathy, K. V.; Kulkarni, G. U.; Rao, C. N. R. A novel method of preparing thiol-derivatised nanoparticles of gold, platinum and silver forming superstructures. *J. Chem. Soc., Chem. Commun.* **1997**, 537–538.
  - (17) Henglein, A.; Meisel, D. Spectrophotometric Observations of the Adsorption of Organosulfur Compounds on Colloidal Silver Nanoparticle. *J. Phys. Chem. B* **1998**, *102*, 8364–8366.
  - (18) Kreibig, U.; Gartz, M.; Hilger, A.; Hovel, H. Mie-plasmon spectroscopy: A tool of surface science. In *Fine Particles Science and Technology*; Pelizzatti, E., Ed.; Kluwer Academic Publishers: Boston, 1996; pp 499–516.
  - (19) Fujiwara, H.; Yanagida, S.; Kamat, P. V. Visible laser induced fusion and fragmentation of thionicotinamide capped gold nanoparticles. *J. Phys. Chem. B* **1999**, *103*, 2589–2591.
  - (20) George Thomas, K.; Zajicek, J.; Kamat, P. V. Surface Binding Properties of Tetraoctylammonium Bromide Capped Gold nanoparticles. *Langmuir* **2002**, *18*, 3722–3727.
  - (21) George Thomas, K.; Kamat, P. V. Making Gold Nanoparticles Glow. Enhanced Emission from a Surface Bound Probe. *J. Am. Chem. Soc.* **2000**, *122*, 2655–2656.
  - (22) Chen, M. M. Y.; Katz, A. Steady-State Fluorescence-Based Investigation of the Interaction between Protected Thiols and Gold Nanoparticles. *Langmuir* **2002**, *18*, 2413–2420.
  - (23) Lee, P. C.; Meisel, D. Adsorption and surface-enhanced Raman of dyes on silver and gold sols. *J. Phys. Chem.* **1982**, *86*, 3391–3395.
  - (24) Kerker, M. Electromagnetic model for surface-enhanced Raman scattering (SERS) on metal colloids. *Acc. Chem. Res.* **1984**, *17*, 271–277.
  - (25) Franzen, S.; Folmer, J. C. W.; Glomm, W. R.; O'Neal, R. Optical properties of dye molecules adsorbed on single gold and silver nanoparticles. *J. Phys. Chem. A* **2002**, *106*, 6533–6540.
  - (26) Nikoobakht, B.; El-Sayed, M. A. Surface-enhanced Raman scattering studies on aggregated gold nanorods. *J. Phys. Chem. A* **2003**, *107*, 3372–3378.
  - (27) Emory, S. R.; Nie, S. M. Near-Field Surface-Enhanced Raman Spectroscopy on Single Silver Nanoparticles. *Anal. Chem.* **1997**, *69*, 2631.
  - (28) Haes, A. J.; Van Duyne, R. P. A nanoscale optical biosensor: Sensitivity and selectivity of an approach based on the localized surface plasmon resonance spectroscopy of triangular silver nanoparticles. *J. Am. Chem. Soc.* **2002**, *124*, 10596–10604.
  - (29) Liu, D.; Kamat, P. V. Electrochemically active nanocrystalline SnO<sub>2</sub> films. Surface modification with thiazine and oxazine dye aggregates. *J. Electrochem. Soc.* **1995**, *142*, 835–839.
  - (30) Nasr, C.; Liu, D.; Hotchandani, S.; Kamat, P. V. Dye capped semiconductor colloids. Excited state and photosensitization aspects of Rhodamine 6G–H aggregates electrostatically bound to SiO<sub>2</sub> and SnO<sub>2</sub> Colloids. *J. Phys. Chem.* **1996**, *100*, 11054–11061.
  - (31) Hranisavljevic, J.; Dimitrijevic, N. M.; Wurtz, G. A.; Wiederrecht, G. P. Photoinduced Charge Separation Reactions of J-Aggregates Coated on Silver Nanoparticles. *J. Am. Chem. Soc.* **2002**, *124*, 4536–4537.
  - (32) Kerker, M. The optics of colloidal silver: Something old and something new. *J. Colloid Interface Sc.* **1985**, *105*, 297.
  - (33) Chandrasekharan, N.; Kamat, P. V.; Hu, J.; Jones, G., II. Dye Capped Gold Nanoclusters: Photoinduced changes in Gold/Rhodamine 6G Nanoassemblies. *J. Phys. Chem. B* **2000**, *104*, 11103–11109.
  - (34) Drexhage, K. H.; Kuhn, H.; Shafer, F. P. Variation of the fluorescence decay time of a molecule in front of a mirror, metal, energy transfer. *Ber. Bunsen-Ges. Phys. Chem.* **1968**, *72*, 329.
  - (35) Ishida, A.; Sakata, Y.; Majima, T. Surface plasmon excitation of a porphyrin covalently linked to a gold surface. *J. Chem. Soc., Chem. Commun.* **1998**, 57–58.
  - (36) Saito, K. Quenching of excited J aggregates on metals by surface plasmon excitations. *J. Phys. Chem. B* **1999**, *103*, 6579–6583.
  - (37) Pagnot, T.; Barchiesi, D.; Tribillon, G. Energy transfer from fluorescent thin films to metals in near-field optical microscopy: Comparison between time-resolved and intensity measurements. *Appl. Phys. Lett.* **1999**, *75*, 4207–4209.
  - (38) Ipe, B. I.; George Thomas, K.; Barazzouk, S.; Hotchandani, S.; Kamat, P. V. Photoinduced Charge Separation in a Fluorophore-Gold Nanoassembly. *J. Phys. Chem. B* **2002**, *106*, 18–21.
  - (39) Kamat, P. V.; Barazzouk, S.; Hotchandani, S. Electrochemical Modulation of Fluorophore Emission at a Nanostructured Gold Film. *Angew. Chem., Int. Ed.* **2002**, *41*, 2764–2767.
  - (40) Stellacci, F.; Bauer, C. A.; Meyer-Friedrichsen, T.; Wenseleers, W.; Marder, S. R.; Perry, J. W. Ultrabright supramolecular beacons based on the self-assembly of two-photon chromophores on metal nanoparticles. *J. Am. Chem. Soc.* **2003**, *125*, 328–329.
  - (41) Imahori, H.; Arimura, M.; Hanada, T.; Nishimura, Y.; Yamazaki, I.; Sakata, Y.; Fukuzumi, S. Photoactive three-dimensional monolayers: Porphyrin-alkanethiolate-stabilized gold clusters. *J. Am. Chem. Soc.* **2001**, *123*, 335–336.
  - (42) Templeton, A. C.; Cliffl, D. E.; Murray, R. W. Redox and fluorophore functionalization of water soluble. tioponin-protected gold clusters. *J. Am. Chem. Soc.* **1999**, *121*, 7081–7089.
  - (43) Thomas, J. K. Characterization of surfaces by excited states. *J. Phys. Chem.* **1987**, *91*, 267–76.
  - (44) Hu, J.; Zhang, J.; Liu, F.; Kittredge, K.; Whitesell, J. K.; Fox, M. A. Competitive photochemical reactivity in a self-assembled monolayer on a colloidal gold cluster. *J. Am. Chem. Soc.* **2001**, *123*, 1464–1470.
  - (45) Dulkeith, E.; Morteani, A. C.; Niedereichholz, T.; Klar, T. A.; Feldmann, J.; Levi, S. A.; van Veggel, F. C. J. M.; Reinhoudt, D. N.; Moller, M.; Gittins, D. I. Fluorescence quenching of dye molecules near gold nanoparticles: Radiative and nonradiative effects. *Phys. Rev. Lett.* **2002**, *89*, 203002.
  - (46) Sudeep, P. K.; Ipe, B. I.; George Thomas, K.; George, M. V.; Barazzouk, S.; Hotchandani, S.; Kamat, P. V. Fullerene Functionalized Gold Nanoparticles. A Self-Assembled Photoactive Antenna-Metal Nanocore Assembly. *Nano Lett.* **2002**, *2*, 29–35.
  - (47) George Thomas, K.; Biju, V.; George, M. V.; Guld, D. M.; Kamat, P. V. Photoinduced Charge Separation and Stabilization in Clusters of a Fullerene-Aniline Dyad. *J. Phys. Chem. B* **1999**, *103*, 8864–8869.
  - (48) Biju, V.; Barazzouk, S.; Thomas, K. G.; George, M. V.; Kamat, P. V. Photoinduced electron transfer between 1,2,5-triphenylpyrroliidino fullerene cluster aggregates and electron donors. *Langmuir* **2001**, *17*, 2930–2936.
  - (49) Brust, M.; Kiely, C. J.; Bethell, D.; Schiffrin, D. J. C-60 mediated aggregation of gold nanoparticles. *J. Am. Chem. Soc.* **1998**, *120*, 12367–12368.
  - (50) Huang, T.; Murray, R. W. Quenching of [Ru(bpy)<sub>3</sub>](<sup>2+</sup>) fluorescence by binding to Au nanoparticles. *Langmuir* **2002**, *18*, 7077–7081.
  - (51) Gu, T.; Whitesell, J. K.; Fox, M. A. Energy Transfer from a Surface-Bound Arene to the Gold Core in  $\omega$ -Fluorenyl-Alkane-1-Thiolate Monolayer-Protected Gold Clusters. *Chem. Mater.* **2003**, *15*, 1358–1366.
  - (52) Aguila, A.; Murray, R. W. Monolayer-protected clusters with fluorescent dansyl ligands. *Langmuir* **2000**, *16*, 5949–5954.
  - (53) Fan, C. H.; Wang, S.; Hong, J. W.; Bazan, G. C.; Plaxco, K. W.; Heeger, A. J. Beyond superquenching: Hyper-efficient energy transfer from conjugated polymers to gold nanoparticles. *Proc. Natl. Acad. Sci. U.S.A.* **2003**, *100*, 6297–6301.

- (54) Maxwell, D. J.; Taylor, J. R.; Nie, S. M. Self-assembled nanoparticle probes for recognition and detection of biomolecules. *J. Am. Chem. Soc.* **2002**, *124*, 9606–9612.
- (55) Wang, G. L.; Zhang, J.; Murray, R. W. DNA binding of an ethidium intercalator attached to a monolayer-protected gold cluster. *Anal. Chem.* **2002**, *74*, 4320–4327.
- (56) Avouris, P.; Persson, B. N. J. Excited States at Metal Surfaces and Their Nonradiative Relaxation. *J. Phys. Chem.* **1984**, *88*, 837–848.
- (57) Enger, O.; Nuesch, F.; Fibbioli, M.; Echegoyen, L.; Pretsch, E.; Diederich, F. Photocurrent generation at a fullerene self-assembled monolayer-modified gold electrode cast with a polyurethane membrane. *J. Mater. Chem.* **2000**, *10*, 2231–2233.
- (58) Imahori, H.; Norieda, H.; Yamada, H.; Nishimura, Y.; Yamazaki, I.; Sakata, Y.; Fukuzumi, S. Light-Harvesting and Photocurrent Generation by Gold Electrodes Modified with Mixed Self-Assembled Monolayers of Boron-Dipyrin and Ferrocene-Porphyrin-Fullerene Triad. *J. Am. Chem. Soc.* **2001**, *123*, 100–110.
- (59) Chen, S.; Ingram, R. S.; Hostetler, M. J.; Pietron, J. J.; Murray, R. W.; Schaaff, T. G.; Khoury, J. T.; Alvarez, M. M.; Whetten, R. L. Gold Nanoelectrodes of Varied Size: Transition to Molecule-Like Charging. *Science* **1998**, *280*, 2098–2101.
- (60) Hicks, J. F.; Templeton, A. C.; Chen, S.; Sheran, K. M.; Jasti, R.; Murray, R. W.; Debord, J.; Schaaff, T. G.; Whetten, R. L. The Monolayer Thickness Dependence of Quantized Double-Layer Capacitances of Monolayer-Protected Gold Clusters. *Anal. Chem.* **1999**, *71*, 3703–3711.
- (61) Shanghavi, B.; Kamat, P. V. Interparticle electron transfer in metal/semiconductor composites. Picosecond dynamics of CdS capped gold nanoclusters. *J. Phys. Chem. B* **1997**, *101*, 7675–7679.
- (62) Chandrasekharan, N.; Kamat, P. V. Assembling gold nanoparticles as nanostructured films using an electrophoretic approach. *Nano Lett.* **2001**, *1*, 67–70.
- (63) Hens, Z.; Tallapin, D. V.; Weller, H. Breaking and restoring a molecularly bridged metal|quantum dot junction. *Appl. Phys. Lett.* **2002**, *81*, 4245–4247.
- (64) Chen, S.; Murray, R. W. Electrochemical Quantized Capacitance Charging of Surface Ensembles of Gold Nanoparticles. *J. Phys. Chem. B* **1999**, *103*, 9996–10000.
- (65) Hainfeld, J. F.; Powell, R. D. New frontiers in gold labeling. *J. Histochem. Cytochem.* **2000**, *48*, 471–480.
- (66) Nam, J. M.; Park, S. J.; Mirkin, C. A. Bio-barcodes based on oligonucleotide-modified nanoparticles. *J. Am. Chem. Soc.* **2002**, *124*, 3820–3821.
- (67) Demers, L. M.; Mirkin, C. A.; Mucic, R. C.; Reynolds, R. A.; Letsinger, R. L.; Elghanian, R.; Viswanadham, G. A fluorescence-based method for determining the surface coverage and hybridization efficiency of thiol-capped oligonucleotides bound to gold thin films and nanoparticles. *Anal. Chem.* **2000**, *72*, 5535–5541.
- (68) Ipe, B. I.; Mahima, S.; Thomas, K. G. Light-Induced Modulation of Self-Assembly on Spiropyran-Capped Gold Nanoparticles: A Potential System for the Controlled Release of Amino Acid Derivatives. *J. Am. Chem. Soc.* **2003**, *125*, 7174–7175.
- (69) Kuwahara, Y.; Akiyama, T.; Yamada, S. Facile Fabrication of Photoelectrochemical Assemblies Consisting of Gold Nanoparticles and a Tris(2,2'-bipyridine)ruthenium(II)-Viologen Linked Thiol. *Langmuir* **2001**, *17*, 5714–5716.
- (70) Lahav, M.; Gabriel, T.; Shipway, A. N.; Willner, I. Assembly of Zn(II)-porphyrin-bipyridinium dyad and Au–nanoparticle superstructures on conductive surfaces. *J. Am. Chem. Soc.* **1999**, *121*, 258–259.
- (71) Kamat, P. V.; Barazzouk, S.; George Thomas, K.; Hotchandani, S. Electrodeposition of C60 Clusters on Nanostructured SnO<sub>2</sub> Films for Enhanced Photocurrent Generation. *J. Phys. Chem. B* **2000**, *104*, 4014–4017.
- (72) Bethell, D.; Brust, M.; Schiffrin, D. J.; Kiely, C. From monolayers to nanostructured materials: An organic chemist's view of self-assembly. *J. Electroanal. Chem.* **1996**, *409*, 137–143.

AR030030H